

Hybrid Method for Constrained and Unconstrained Trajectory Optimization of Space Transportation

Iman Shafieenejad^{1,*} 

¹.Aerospace Research Institute  – Department of Aeronautics – Ministry of Science Research & Technology – Tehran – Iran.

*Correspondence author: shafieenejad@ari.ac.ir

ABSTRACT

In this research, a new method named δ to solve non-linear constrained and un constrained optimal control problems for trajectory optimization was proposed. The main objective of this method was defined as solving optimal control problems by the combination of the orthogonal functions, the heuristic optimization techniques, and the principles of optimal control theory. Three orthogonal functions Fourier, Chebyshev, and Legendre were considered to approximate the control variables. Also, GA-PSO and imperialist competition algorithms were considered as heuristic optimization techniques. Moreover, the motivation of the mentioned method belonged to a novel combination of zero Hamiltonian in the optimal control theory, optimality conditions, and newly proposed criteria. Furthermore, lunar landing, asteroid rendezvous, and low-thrust orbital transfer with respect to minimum-time and minimum-fuel criteria were investigated to show the ability of the proposed method in regard to constrained and un constrained optimal control problems. Results demonstrated that the δ method has high accuracy in the optimal control theory for non-linear problems. Hence, the δ method allows space trajectory and mission designers to solve optimal control problems with a simple and precise method for future works and studies.

Keywords: Off-on control; Optimal control; Time optimal control; Flight optimization; Chebyshev approximation.

INTRODUCTION

Solving optimal control problems for achieving optimal trajectories was the main focus of many studies up to now. Three steps of solving trajectory optimization problems were classified as mathematical modeling, defining the main criterion, and proposing the method of solving. In this way, one of the most important parts of the mentioned steps was the approach of achieving the optimal solutions regarding the introduction of a precise method. Hence, various methods to solve the optimal control problems were presented with respect to direct, indirect, and the combination of direct and indirect methods in the optimal control theory (Ben-Asher 2010; Chen and Tang 2018; Han *et al.* 2019; Naidu 2003; Shirazi *et al.* 2018). In this study, a combination of direct and indirect optimal control methods was demonstrated. The main contribution of this work belonged to introducing the precise approximation of optimal control by heuristic optimization techniques and orthogonal functions. Regarding the approximation of the optimal control, new augmented criteria based on the optimal control theory were introduced to minimize by optimization techniques. The mentioned augmented criteria was named by the different indices of δ that belonged to the optimal control

Received: Jan 16, 2023 | **Accepted:** June 24, 2023

Section editor: Alison Moraes 

Peer Review History: Single Blind Peer Review.



This is an open access article distributed under the terms of the Creative Commons license.

theory. The main criterion (such as minimum-time or minimum-fuel) was added by new criteria introduced by δ based on the necessary and sufficient conditions in the optimal control theory to improve the precision and simple achievement of the results. However, another reference that review in the bellow didn't consider it. From a different point of view, the introduced method in this work was an open-loop optimal control.

Some research including direct methods. Dynamic programming was one of the basic direct methods to solve optimal control problems (Kirk and Demetry 1971). In this way, collocation discretization regarding the fractional diffusion equation was proposed (Li and Zhou 2019). In Li and Zhou (2019) the necessary optimality condition was derived; however, in this work, necessary and sufficient conditions were studied. Moreover, in Fuica (2019), an artificial bee colony and direct collocation method were proposed for reentry trajectory optimization. The control variables were discretized at a set of Legendre-Gauss collocation points and are optimized with the ABC approach. However, discretization of the optimal control variable caused complicated processes and the current method of this study approximated the optimal control without discretization. Also, Fuica (2019) investigated a new method where the control variables belonged to the regular Borel measures as the posterior error estimator. Discretization of the control variable and the approximation of the state equations were studied. In comparison to this research and Ross (2019), it should be noted that the current research only approximated the optimal control and didn't depend on the approximation of state equations.

Other studies were devoted to indirect methods and their combinations with direct methods. In 2019, a zero-Hamiltonian ($H=0$), from optimal control theory to achieve an indirect method for the trajectory optimization of non-linear problems, was considered in Ross (2019). Furthermore, Sobolev and Lebesgue considered weighted spaces in the horizon optimal control problems by other mathematical approaches such as Legendre and Chebyshev polynomials in Braun *et al.* (2016) and Lykina and Pickenhain (2017). Also, Fourier series, Chebyshev and Legendre polynomials were compared for trajectory optimization of minimum-time and minimum-effort based on the non-constrained optimal control problems Shafieenejad and Novinzadeh (2010) and Shafieenejad *et al.* (2014). However, this study considered minimum-fuel based on the on-off optimal controls for non-linear constraint problems. Pontani *et al.* (2014) investigated trajectory optimization of a spacecraft by the variable time-domain and minimization of the second differential of minimum-time criterion. Hence, Pontani *et al.* (2014) studied two case studies as lunar ascent/descent and circular coplanar transfer regarding indirect methods. Furthermore, Ross (2015) introduced the modern viewpoint of the co-vector mapping principle which connected the missing link between the traditional direct/indirect approaches, this viewpoint had also been noted in Shirazi *et al.* (2018).

One of the main applications of the optimal control theory for optimal trajectory designing was the minimum-fuel criterion which usually causes bang-bang (on-off) controls. Also, bang-bang constrained controls in the optimal control problems led to the complicated non-linear problems referring to the bounded controls (Binfeng *et al.* 2019; Chen *et al.* 2018; Kumar *et al.* 2018; Yan and Zhu 2015; Zhu *et al.* 2017). In this way, a time-stepping method by discontinuous Galerkin method was investigated by Henriques *et al.* (2017a; b). In Henriques' studies, the pseudo-spectral method was enhanced in the bang-bang optimal control problems with the orthogonal functions as sub-optimal solutions. Moreover, optimal control with chattering controls was addressed. Also, in Henrion *et al.* (2019) a new method based on avoiding discontinuities regarding the antistrophic parameterized measures with chattering control was proposed. From another point of view, bang-bang controls had many applications for optimal orbital transfers with respect to the minimum-fuel consumption. An ephemeris model for short and long orbital transfer to the Moon was investigated regarding initial guesses method, however, dependency of methods in initial guesses is not suitable for the optimal control methods (Shafieenejad *et al.* 2015). In this way, one of the advantages of this study belonged to the independence of the proposed δ method to the initial guesses.

Many trajectory optimization problems were categorized in space missions based on the impulsive orbital transfers and low-thrust orbital transfers to the Geosynchronous Earth Orbit (GEO), Moon, and asteroids (AlandiHallaj and Assadian 2019; Lunghi 2017; Udupa *et al.* 2018). So, a rendezvous maneuver regarding multiple missions was addressed regarding the impulsive low-thruster (Gao *et al.* 2019). Gao *et al.* (2019) focused on obtaining solutions by a shape-based polynomial for an optimal low-thrust trajectory. Also, a new method was proposed for a sub-optimal trajectory optimization to investigate an orbital transfer to an asteroid by low-thrust transfer (Bazzocchi and Emami 2018). In this way, Bazzocchi applied the genetic algorithm to introduce a new method regarding global optimization. Moreover, in Quarta and Mengali (2019) a semi-analytical method for orbital transfer

was proposed based on the magnitude of the velocity without any changes in directions. Further, a GA was applied to achieve the minimum changes in the magnitude of velocity. Furthermore, a new method by global optimization technique as GA was proposed to avoid an initial population with several initial guesses (Mohammadi and Naghash 2019). It should be noted, different space missions such as constraint and non-constrained Lunar landing, rendezvous, and low-thrust orbital transfer for different criteria were studied by the proposed method without any initial guesses and optimal control and state equations discretization.

Open-loop and closed-loop methods were two different branches of the optimal control theory. Closed-loop optimal controls were robust against disturbances, however, the open-loop optimal controls were sensitive to the disturbances. Also, the model predictive control could enhance the ability of the system against unknown disturbances. The mentioned method in this research belonged to the open-loop branch of optimal control theory. It should be noted that, usually, to introduce the closed-loop optimal control, first, the open-loop optimal control theory was studied (Naidu 2003). In this way, the application of artificial intelligence and robust methods were studied in the references. In Chai *et al.* (2021) the problem of trajectory optimization for autonomous ground vehicles with the consideration of irregularly placed on-road obstacles and multiple maneuver phases were studied by introducing a series of event sequences. Also, fast trajectory planning by reinforcement learning in an unknown environment was studied in Chai *et al.* (2022a). The application of neural networks to predict the optimal control for the autonomous motion of ground vehicles regarding parking maneuvers was studied by Chai *et al.* (2022b) in. In this way, Chai *et al.* (2022c) see the other reference for deep learning trajectory planning and control for autonomous ground vehicles. In Chai *et al.* (2022d), optimal time-varying with system constraints and considering disturbances for attitude tracking of a spacecraft was demonstrated. The optimal control in Chai *et al.* (2022d) was established by introducing a non-linear robust model predictive control and a dual-loop cascade tracking control framework. Also, the other reference was suggested for model predictive control for a reentry vehicle in Chai *et al.* (2022e).

In this work, a new method will be introduced as a δ method with combination characters of direct and indirect methods. First, this article that follows introduces δ method for optimal control problems regarding optimal control theory, orthogonal functions, and GA-PSO, and Imperialist Competition Algorithm (ICA) optimization techniques. Next, two non-linear problems in space trajectory optimization, the Lunar landing and the asteroid rendezvous are studied. Finally, a low-thrust orbital transfer is investigated regarding minimum-time and minimum-fuel criteria. Minimum-fuel criterion is considered a constrained problem with constant thrust magnitude and multiple on-off optimal controls. Emphasizing on the minimum-time and minimum-fuel criteria and different space missions show the ability of this method for different types of optimal control problems.

BRIEF INTRODUCTION TO OPTIMAL CONTROL THEORY

Optimal Control Problems lead to solving a system of first-order differential equations (Eq. 1). The main goal of the mentioned equations is deriving an optimal control $\mathbf{u}(t)$ to reduce a cost function.

$$\dot{x} = \chi(x(t), u(t), t) \quad (1)$$

where $x(t)$ is the state vector. Therefore, the main cost function J_m is demonstrated by Eq. 2:

$$J_m = \int_0^{t_f} \vartheta(x(t), u(t), t) dt + \phi(x(t_f)) \quad (2)$$

In the equation above, $\phi(x(t_f))$ is the final condition of the main cost function. With respect to the optimal control theory, Hamiltonian of the system in Eq. 1 is introduced by Eq. 3.

$$H = \vartheta(x(t), u(t), t) + \lambda(t)\chi(t) \quad (3)$$

$\lambda(t)$ is considered as the co-state vector and achieved as (Eq. 4):

$$\dot{\lambda}(t) = \frac{-\partial H}{\partial x(t)} \quad (4)$$

Also, the optimality condition regarding the Hamiltonian of the system is introduced in Eq. 5 (Naidu 2003).

$$\frac{\partial H}{\partial u(t)} = 0 \quad (5)$$

Optimal control problems with non-differentiating control functions (constrained control) cover a wide range of optimal trajectory designing. Also, some of the constrained optimal control problems are called “bang-bang” because of the on-off control functions. Hence, optimal control $u(t)$ is obtained with respect to satisfying the following inequality (Eq. 6).

$$H(x^*(t), \lambda^*(t), u^*(t), t) \leq H(x^*(t), \lambda^*(t), u(t), t) \quad (6)$$

$H(t)$ is the Hamiltonian function and $x(t)$, $\lambda(t)$, $u(t)$ are states, co-states, and optimal controls respectively. Also, ‘*’ is referred to as the optimal parameter. Since $u(t)$ is discrete in the bang-bang problems, the optimality condition $\partial H/(\partial u(t))=0$ cannot be used. So, $u(t)$ is considered by Eq. 7.

$$u(t) = u^*(t) = \{u_{min} \zeta_s(t) > 0 \quad u_{max} \zeta_s(t) < 0 \quad (7)$$

The sign of switch function $\zeta_s(t)$ has an important role in the bang-bang problems.

METHOD

In the δ method proposed in this study, a combination of direct and indirect optimal control methods was considered. In the mentioned method, the precise approximation of optimal control by heuristic optimization techniques and orthogonal functions is introduced. Regarding the approximation of the optimal control, new augmented criteria based on the optimal control theory were introduced to minimize by the optimization techniques. The mentioned augmented criteria were named by the different indices of δ that belonged to the optimal control theory. The main criterion (such as minimum-time or minimum-fuel) was added by new criteria introduced by δ based on the necessary and sufficient conditions in the optimal control theory to improve the precision and simple achievement of the results.

In the proposed δ method, switch function is considered through orthogonal functions by Eq. 8:

$$f_s(t) = \sum_{i=1}^N \pi_i \zeta_i(t) \quad (8)$$

where $\zeta_i(t)$ and π_i are the orthogonal functions and multipliers of the estimated switch function respectively. Switch function f_s can be achieved regarding optimal determining $\zeta_i(t)$ and π_i , where i is the index of the components. Heuristic optimizer determines the optimal multipliers π_i for the best $f_s(t)$. Also, based on the positive or negative value of $f_s(t)$, control variable $u^*(t)$ is achieved.

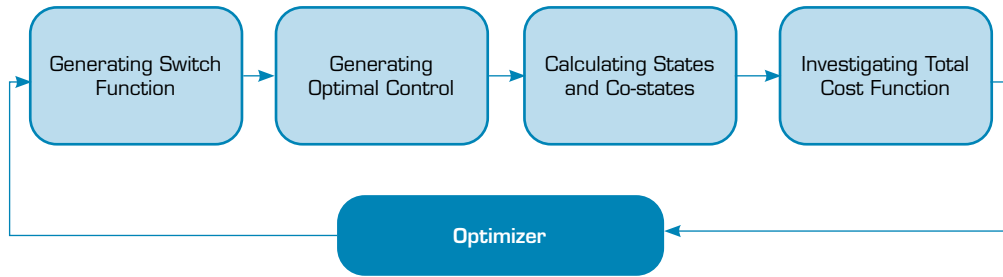
When $f_s(t)$ (switch function) and $u^*(t)$ (optimal control) are approximated by the orthogonal functions, states and co-states $dx/dt=(\partial H(t))/(\partial \lambda(t))$, $d\lambda/dt=-(\partial H(t))/(\partial x(t))$ could be integrated with respect to initial conditions. An augmented cost function (see Eq. 9) is defined based on the terminal conditions and states at the end of the trajectory.

$$J_a = \sum_{j=1}^M \frac{k_j}{2} [x^j_{nominal}(t) - x^j(t)]_{t_f}^2 \quad (9)$$

where j is the index of terminal conditions and k is the weight coefficients. Hence, the optimizer minimize the J_a and the final-conditions are satisfied.

The main cost function J_m (such as minimum-time or minimum-fuel), augmented cost function J_a (Eq. 9) that belongs to the satisfaction of state equations at the end) will be obtained. Next, criteria δ from δ method, will be explained to construct the total cost function J_{total} .

Main process of δ method to solve optimal control problems is considered via powerful heuristic optimizers. Regarding Fig. 1, optimizer chooses a suitable switch function through the best π_i which has reduced J_{total} . This process is continued through iterative loop of optimizer to reduce J_{total} .



Source: Elaborated by the authors.

Figure 1. δ method main algorithm.

Components of criteria δ are explained step by step in the following (Eq. 10).

First, δ_s^H is defined in below equations. From Eq. 6:

$$H(x^*(t), \lambda^*(t), u^*(t)) - H(x^*(t), \lambda^*(t), u(t)) \leq 0 \quad (10)$$

So, δ_s^H is defined as (Eq. 11):

$$\delta_s^H = \int_0^{t_f} [H_i(t) - H_{i-1}(t)] dt \quad (11)$$

In the above formula, $(i - 1)$ indicates the previous iteration of the optimization process. Optimizer selects the better multipliers of orthogonal functions in order to achieve the best control regarding satisfying inequality (Eq. 10). So, the Hamiltonian is reduced and will be smaller in every iteration when $\delta_s^H \rightarrow 0$ (see Eqs. 10 and 11).

Second, δ_s^H regarding the switch function is defined. In this way, Hamiltonian can be stated as follow (Eq. 12):

$$H(t) = \sigma(x(t), \lambda(t)) + \eta(x(t), \lambda(t), u(t)) \quad (12)$$

where $\eta(t)$ is the other part of Hamiltonian that has $u(t)$ (Eq. 13).

$$\eta(t) = g(u(t)) \cdot \zeta(x(t), \lambda(t)) \quad (13)$$

So, $f_s^I(t)$ is considered as (Eq 14):

$$f_s^I(t) = \zeta(x(t), \lambda(t)) \quad (14)$$

The best switch function is achieved regarding minimizing the difference between $f_s(t)$ and $f_s^I(t)$. Hence, δ_s^I is defined in Eq. 15 to be minimized to zero $\delta_s^I \rightarrow 0$.

$$\delta_s^I = \int_0^{t_f} |f_s(t) - f_s^I(t)| dt \quad \delta_s^I \rightarrow 0 \quad (15)$$

So, δ_s^I and δ_s^H are taken into account as sub-criteria in the process of optimization. Therefore, optimizer not only minimize J_{total} as well as J_a but also, it minimize δ_s^H and δ_s^I to zero.

Third, δ_u regarding changing in the Hamiltonian with respect to an unconstrained control variable $u(t)$ is defined. Hamiltonian is differentiable when a control variable acts continuously as $u(t)$. Therefore, $(\partial H(t))/(\partial u(t))$ should converge to zero. So, δ_u is defined by Eq. 16:

$$\delta_u = \int_0^{t_f} \left| \frac{\partial H(t)}{\partial u(t)} \right| dt \quad \delta_u \rightarrow 0 \quad (16)$$

As δ_u is minimized to zero, the new criterion is also taken into account. Finally, the total criterion (or cost function) is expressed by Eq. 17 or 18:

$$J_{total} = K_a \cdot J_a + k_m J_m + k_s^H \delta_s^H + k_s^I \delta_s^I + k_u \delta_u \quad (17)$$

or

$$J_{total} = K \cdot J \quad (18)$$

where, $K = [K_a, k_m, k_s^H, k_s^I, k_u]$ is a weight vector and $J = [J_a, J_m, \delta_s^H, \delta_s^I, \delta_u]$.

Fourth, Free-Final-Time problems: Solving the optimal control problem is more difficult when the final-time is free and the control variable is constrained. To make this problem easier, final-time is supposed t_d . In this way, t_d is considered as the approximation of final time t_f by the path planning designer. So t_d is determined $t_d = Ct_f$ and the optimizer will find the best coefficient of c . In a case of free-final-time of optimal control problems, the Eq. 19 can be used for the problems from transversality in the optimal control theory.

$$\left[H(t) + \frac{\partial \Phi(t)}{\partial t} \right]_{t_f} = 0 \quad (19)$$

$\Phi(t)$ indicates terminal section of the main criterion. If $(\partial \Phi(t))/\partial t = 0$, the Hamiltonian will be equal to zero in the final-time $H(t) = 0$. The Hamiltonian variations with respect to the time will equal to zero in the optimal control problems, when the state equations are not explicitly functions of time (see Naidu 2003). Therefore, Eqs. 20 and 21 are resulted.

$$\frac{\partial H(t)}{\partial t} = \frac{dH(t)}{dt} \quad (20)$$

$$\frac{dH(t)}{dt} = 0 \Rightarrow H(t) = cte \quad (21)$$

Since $H(t) = cte$ and $H(t) = 0$, then it can be concluded that the Hamiltonian equals to zero over the time of optimal control problem so, $H(t) = 0$. In the problems of free-final-time, the Eq. 22 criterion is added to the total cost function.

$$\delta_H = \int_0^{t_f} |H(t)| dt \quad \delta_H \rightarrow 0 \quad (22)$$

As δ_H is minimized to zero, some other principles of optimal control theory are considered in solving free-final-time problems regarding the δ method.

If $(\partial \Phi(t))/\partial t \neq 0$, then the Eqs. 23 and 24 inequality is used and δ_H' criterion is defined.

$$\left| H(t) + \frac{\partial \Phi(t)}{\partial t} \right| \leq |H(t)| + \left| \frac{\partial \Phi(t)}{\partial t} \right| \quad (23)$$

$$\delta'_H = \int_0^{t_f} |H(t)| dt + \int_0^{t_f} \left| \frac{\partial \Phi(t)}{\partial t} \right| dt \quad \delta'_H \rightarrow 0 \quad (24)$$

So, the total cost function will be considered by Eq. 25:

$$J_{tot} = K_a \cdot J_a + k_m J_m + k_s^H \delta_s^H + k_s^I \delta_s^I + k_u \delta_u + (k_H \delta_H \text{ or } k'_H \delta'_H) \quad (25)$$

The mentioned issues represent a novel method for optimal control problems with un constrained and constrained control variables.

SOFT LANDING

This simple benchmark investigates the soft landing of a Moon lander. Soft landing of a vehicle with discontinuous optimal control is investigated with the δ method and the mentioned problem is formulated as a constrained optimal control problem. At the end of the mission to the Moon, the lander has a soft landing through the reverse thrust. In Naidu (2003) and Udupa *et al.* (2018) this problem is formulated with respect to minimum-time criterion with on-off optimal control. With reference to the Cartesian coordinate, dynamic equations of the Moon lander are given by Eqs. 26–28:

$$\frac{dy}{dt} = v(t) \quad (26)$$

$$\frac{dv}{dt} = -g_{Moon} + \frac{\kappa}{m(t)} u(t) \quad (27)$$

$$\frac{dm}{dt}(t) = u(t) \quad (28)$$

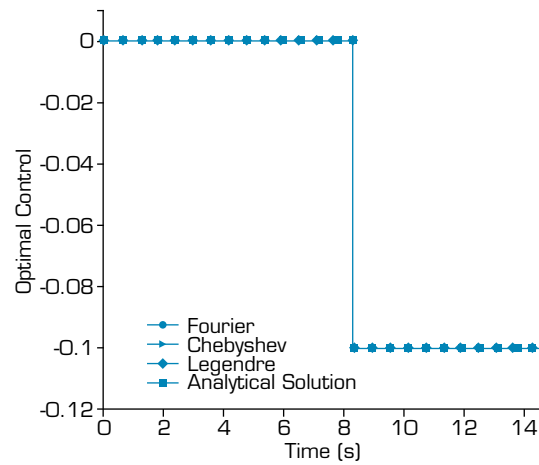
with initial conditions (Eq. 29):

$$y(t_0) = 200(m), v(t_0) = 0\left(\frac{m}{s}\right), m(t_0) = 20(kg) \quad (29)$$

where $v(t)$ is the vertical velocity and g_{Moon} is the gravitational acceleration of the moon. κ is a constant that refers to the exhaust coefficient of the thruster and m is the mass of the lander. Thrust, vector T is upward to the Moon surface and its magnitude is $|T^\rightarrow| = \kappa(dm/dt)$ and dm/dt is the mass reduction rate. Also, the on-off control is represented by u . For a soft landing, the Eq. 30 terminal conditions are satisfied.

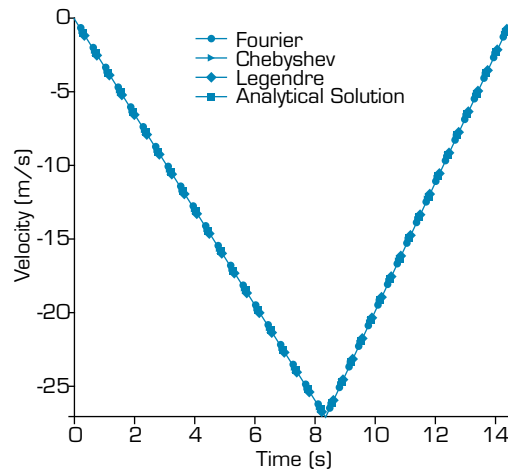
$$y(t_f) = 0(m), v(t_f) = 0\left(\frac{m}{s}\right), m(t_f) = free(kg) \quad (30)$$

The main part of solving this optimal control problem is determining discontinuous optimal control regarding three orthogonal functions: Fourier, Chebyshev, and Legendre. Figures 2–5 represent the Fourier, Chebyshev and Legendre solutions for the optimal control, velocity, height, and mass. In this way, the optimizer chooses the best coefficients for the mentioned three orthogonal functions to construct control switch functions.



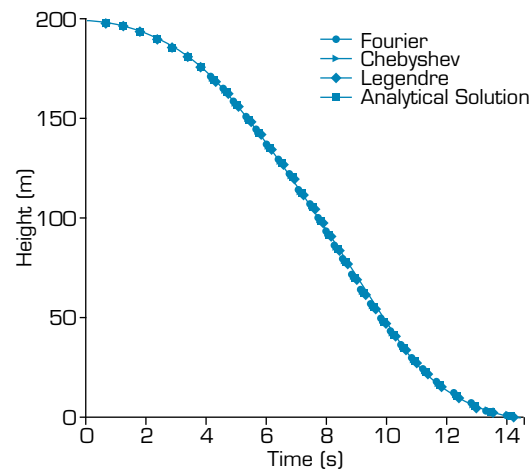
Source: Elaborated by the authors.

Figure 2. Lunar lander on-off optimal control, Fourier, Chebyshev, Legendre results.



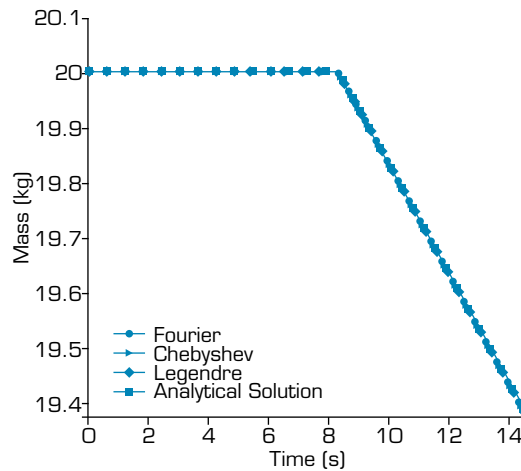
Source: Elaborated by the authors.

Figure 3. Lunar lander velocity, Fourier, Chebyshev, Legendre results.



Source: Elaborated by the authors.

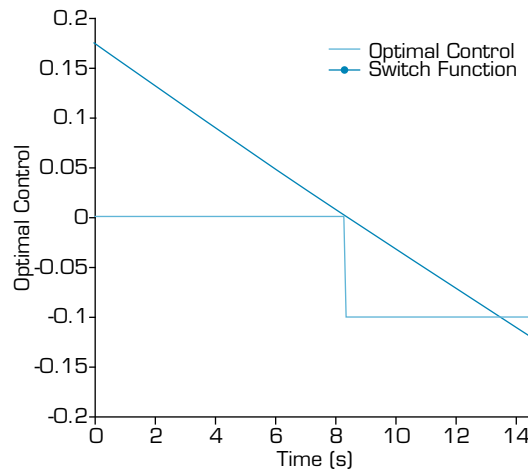
Figure 4. Lunar lander height, Fourier, Chebyshev, Legendre results.



Source: Elaborated by the authors.

Figure 5. Lunar lander mass reduction, Fourier, Chebyshev, Legendre results.

Also, Fig. 3 and 4 show that the boundary conditions are satisfied exactly and state equations have precise results with respect to the analytical solutions in Naidu (2003). Moreover, Fig. 5 represents the mass reduction and it shows the reduction in mass when the thruster is operating based on the switching time. Figure 6 demonstrates on-off optimal control regarding the switch function achieved from δ method.

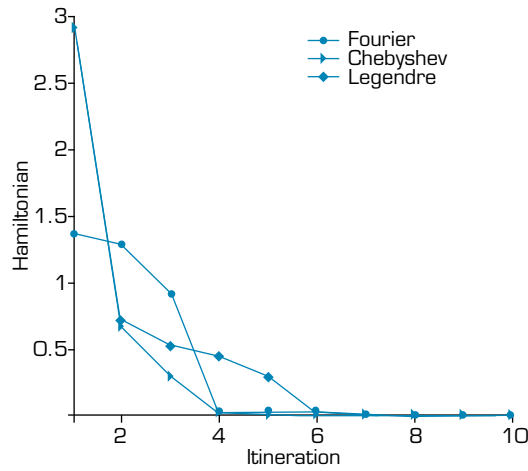


Source: Elaborated by the authors.

Figure 6. Lunar lander on-off optimal control and switch function.

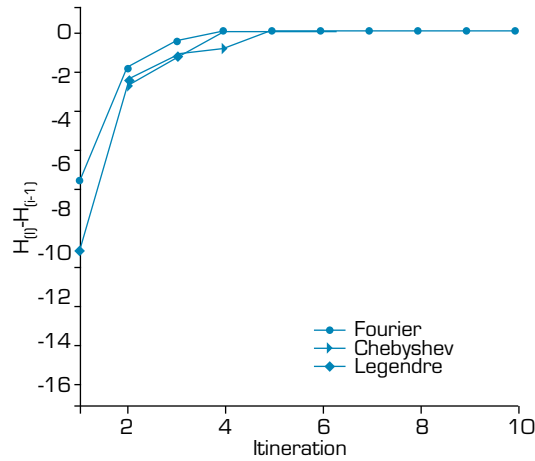
Figures 7–9 demonstrate the robustness and rapid converging of results with respect to the proposed δ method to meet the mentioned method.

The novel parts were introduced in this method as criteria are δ_{HP} , δ_s^H and δ_s^I . Based on the δ method, these parameters are minimized to zero to satisfy the principles of δ method and optimal control theory. Hence, Figs. 7–9 show $S_{Moon} = [\delta_H \delta_s^H \delta_s^I]$ converging to zero rapidly. Finally, in Fig. 10 the reduction of the total cost function is illustrated by three orthogonal functions. It is concluded that the Fourier series has rapid convergence and is considered the best orthogonal function for the δ method. Moreover, to investigate the robustness of the algorithm, ICA is considered for the next optimization technique. So, the next figures are investigating two optimizers GA-PSO and ICA to show the accuracy of the δ method and converging speed. Also, the parameters of the optimizers are illustrated in Table 1. For more references in ICA optimization technique see Abdollahi *et al.* (2013), Ardalan *et al.* (2015), Maheri and Talezadeh (2018) and Rabiee *et al.* (2018). It should be noted, parameters of optimizers in Table 1 are considered by try and errors regarding converging the total cost (see Fig. 10).



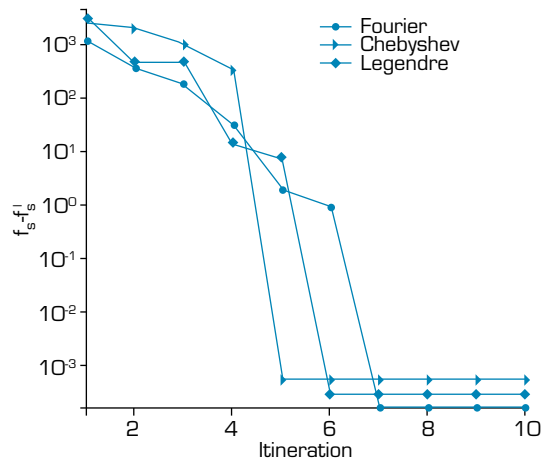
Source: Elaborated by the authors.

Figure 7. Reduction of Hamiltonian criterion δ_H for Fourier, Chebyshev, Legendre w.r.t iterations.



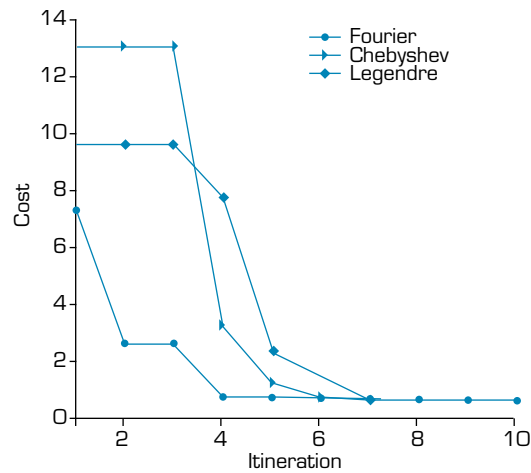
Source: Elaborated by the authors.

Figure 8. Reduction of δ_s^H for Fourier, Chebyshev, Legendre w.r.t iterations.



Source: Elaborated by the authors.

Figure 9. Reduction of δ_s^I for Fourier, Chebyshev, Legendre w.r.t iterations.



Source: Elaborated by the authors.

Figure 10. Reduction of the total cost function, for Fourier, Chebyshev, Legendre w.r.t iterations.

Table 1. Parameters of optimizers.

ICA Parameters		GA-PSO Parameters	
Number of initial countries	5000	Population Size	5000
Number of Initial Imperialist	20	Keep Percent	40/100
Number of decades	10	Cross Percent	40/100
Revolution Rate	0.3	Mutation Percent	5/100
Assimilation Coefficient	2		
Assimilation Angle Coefficient	0.5	Selection Mode	Tournament Selection

Source: Elaborated by the authors.

Figures 11–18 show the precise results of two powerful optimization techniques (GA-PSO, ICA). However, from processing time and rapid converging in Figs. 15–18, the combination of the Fourier series and the GA-PSO optimizer is a candidate (see Table 2). Also, the vector of optimization variables is defined in range $[-\pi\pi]$ and switch functions are obtained as follows (Eqs. 31–34):

Fourier series. GA-PSO

$$f_s(t) = 0.74486 \sin(0.0027339 t) - 1.2623 \sin(0.0082017 t) - 0.42484 \sin(0.0054678 t) - 0.084165 \sin(0.010936 t) - 0.7293 \sin(0.013669 t) + 0.17938 \quad (31)$$

Chebyshev series. GA-PSO

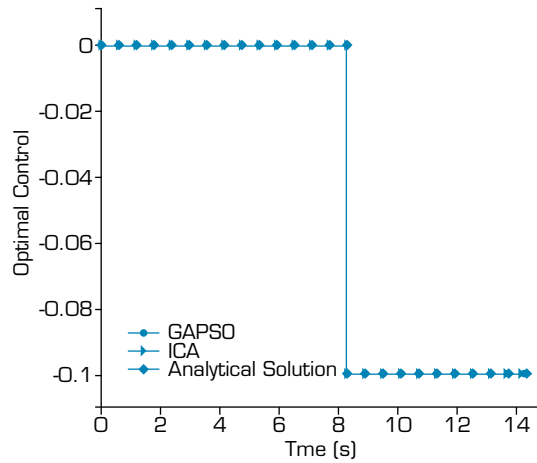
$$f_s(t) = -2.2841e - 9t^5 + 1.0808e - 6t^4 - 0.00017718t^3 + 0.011816t^2 - 0.27478t + 0.17202 \quad (32)$$

Legendre series. GA-PSO

$$f_s(t) = -8.5881e - 10t^5 + 4.23e - 7t^4 - 0.000070026t^3 + 0.0044956t^2 - 0.089034t + 0.049576 \quad (33)$$

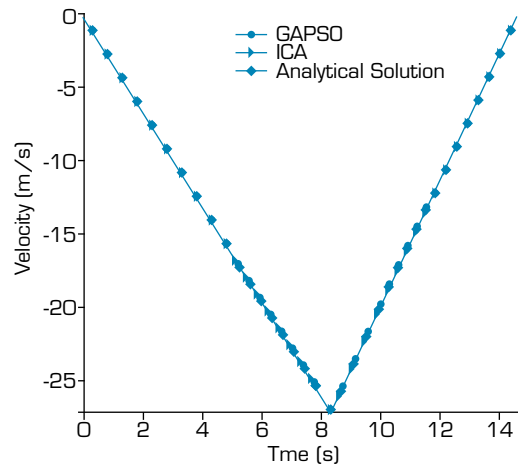
Fourier series. ICA

$$f_s(t) = 0.24675 - 1.2231 \sin(0.0051025 t) - 0.15095 \sin(0.010205 t) - 1.5 \sin(0.012756 t) - 0.3287 \sin(0.0076537 t) - 0.069719 \sin(0.0025512 t) \quad (34)$$



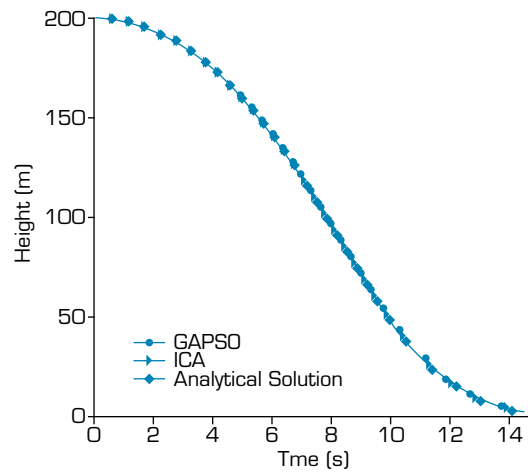
Source: Elaborated by the authors.

Figure 11. Lunar lander on-off optimal control, GA-PSO and ICA results.



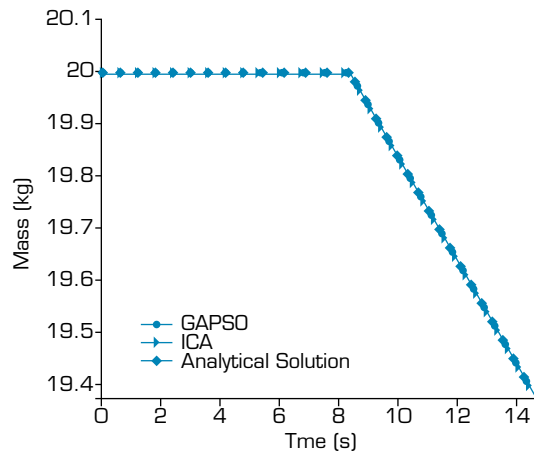
Source: Elaborated by the authors.

Figure 12. Lunar lander velocity, GA-PSO and ICA results.



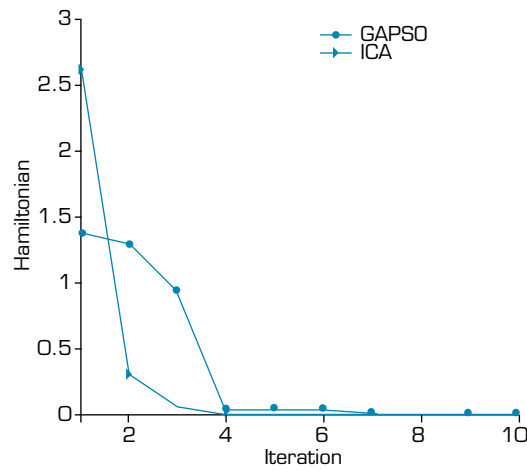
Source: Elaborated by the authors.

Figure 13. Lunar lander height, GA-PSO and ICA results.



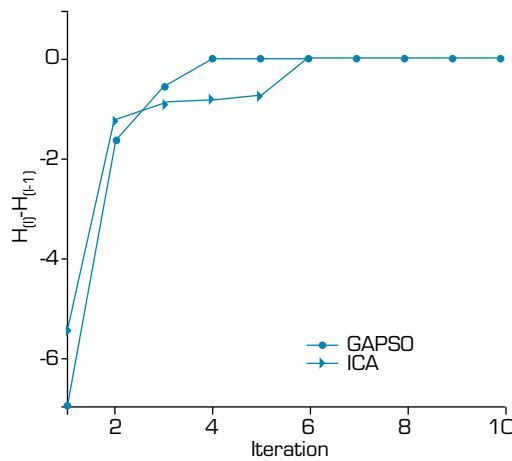
Source: Elaborated by the authors.

Figure 14. Lunar lander mass reduction, GA-PSO and ICA results.



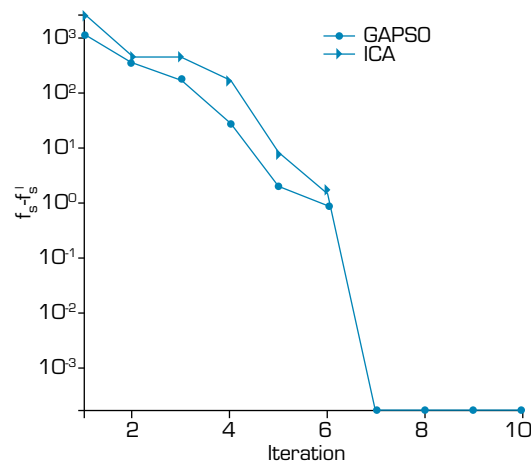
Source: Elaborated by the authors.

Figure 15. Reduction of the Hamiltonian, GA-PSO and ICA results.



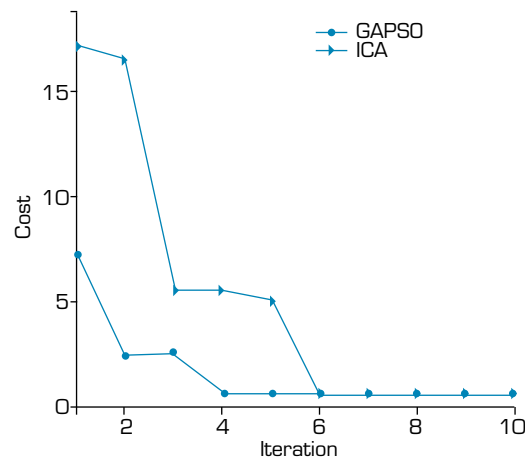
Source: Elaborated by the authors.

Figure 16. Reduction of δ_s^H , GA-PSO and ICA results.



Source: Elaborated by the authors.

Figure 17. Reduction of δ_s^l , GA-PSO and ICA results.



Source: Elaborated by the authors.

Figure 18. Reduction of total cost function, GA-PSO and ICA results.

It is concluded, the coefficients of the series are in range $[-\pi\pi]$. Also, final-time for the minimum-time of the soft lunar lander problem is achieved at 14.6 (s) and the switching occurs at 8.3 (s) for the Fourier series and the GA-PSO results.

Table 2. Comparing processing time.

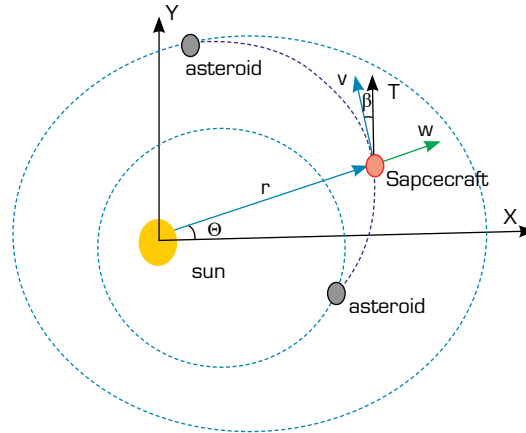
Fourier series & GA-PSO Optimizer	91.73 (sec)
Legendre series & GA-PSO Optimizer	187.16 (sec)
Chebyshev series & GA-PSO Optimizer	145.89 (sec)
Fourier series & ICA Optimizer	268.05 (sec)

Source: Elaborated by the authors.

Fixed Final-Time Problem: Asteroid Rendezvous

The Asteroid Rendezvous problem is about finding the best solution to an interplanetary trajectory problem. The mentioned problem is considered as designing a planar optimal trajectory that starts from an asteroid and intercepts with another asteroid. The mathematical formulation is demonstrated in the solar-centric polar coordinate. The control variable

is represented by $\beta(t)$. The control variable is the angle between the bang-bang thruster and the local horizon. The system of equations for this orbital transfer is represented by five state equations: r , θ , u , v and m . States r and θ are belonged to the position in polar coordinate and u , v are radial and tangential velocities (see Fig. 19). Also, the mass for this transfer is m and it is reduced by $\dot{m} = -T/(I_{sp} g_0)$.



Source: Elaborated by the authors.

Figure 19. Schematic asteroid transfer in the Solar-centric polar coordinate.

The non-linear equations for the spacecraft are considered by Eqs. 35–39:

$$\frac{dr}{dt} = w \quad (35)$$

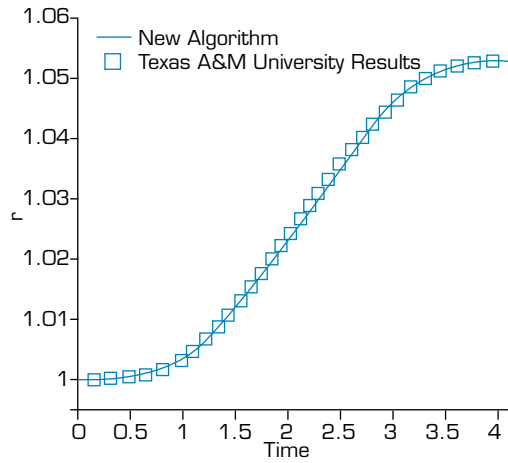
$$\frac{d\theta}{dt} = \frac{v}{r} \quad (36)$$

$$\frac{du}{dt} = \frac{v^2}{r} - \frac{\mu_{\odot}}{r^2} + \frac{T}{m} \sin \beta \cos \beta \quad (37)$$

$$\frac{dv}{dt} = -\frac{wv}{r} + \frac{T}{m} \cos \beta \sin \beta \quad (38)$$

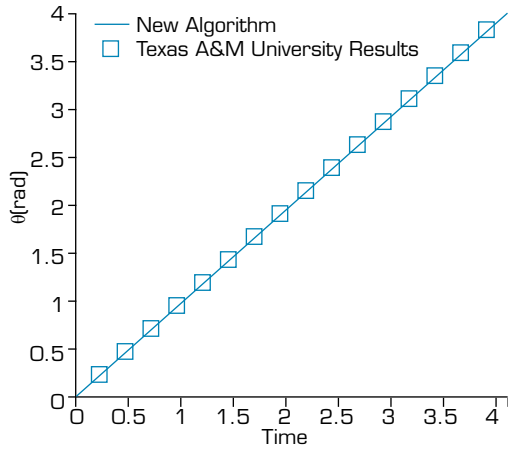
$$\frac{dm}{dt} = -\frac{T}{I_{sp} g_0} \quad (39)$$

The magnitude of the thruster is in the form of bang-bang and considered T_{min} and T_{max} . The specific impulse is $I_{sp} = 3000(s)$ and the initial mass of the spacecraft is $m_0 = 1500(kg)m_0$. The main cost function of the problem is minimum-fuel with fixed-final-time of 240 days. Also, normalized initial and final conditions for this rendezvous problem are considered as $[r_0 = 1, \theta_0 = 0, v_0 = 0, u_0 = 0, m_0 = 1]$ and $[r_f = 1.05243, \theta_f = 3.99192, v_f = 0.97477, u_f = 0, m_f = free]$. Mentioned boundary conditions are non-dimensionalized by these solar parameters as $1AU = 1.49598 \times 10^{11} (m)$ and $1TU = 5.02265 \times 10^6 (s)$. Also, mass is non-dimensionalized by the initial mass of the spacecraft. Maximum thrust is achieved non-dimensionally as T_{max} . Moreover, the mass reduction rate and the final-time are non-dimensionalized as $dm/dt = -0.01536$ and $t_f = 4.1285$. The results of this problem are demonstrated through Figs. 20–31 regarding δ method.



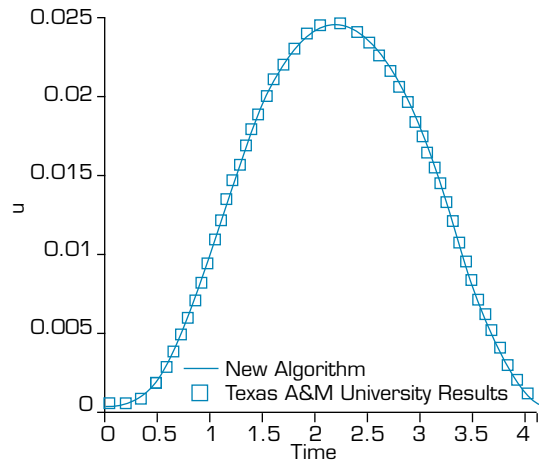
Source: Elaborated by the authors.

Figure 20. Non-dimensionalized radial distance.



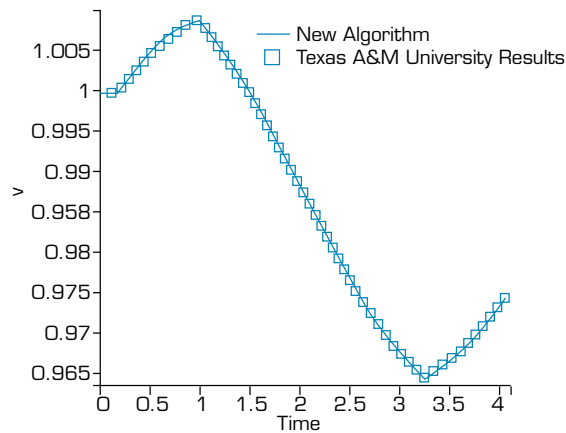
Source: Elaborated by the authors.

Figure 21. Angular parameters in the polar coordinate.



Source: Elaborated by the authors.

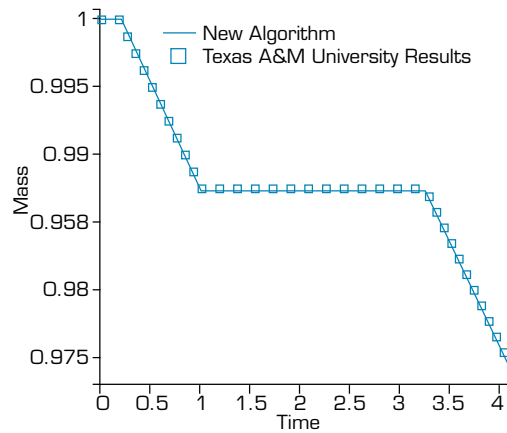
Figure 22. Non-dimensionalized radial velocity.



Source: Elaborated by the authors.

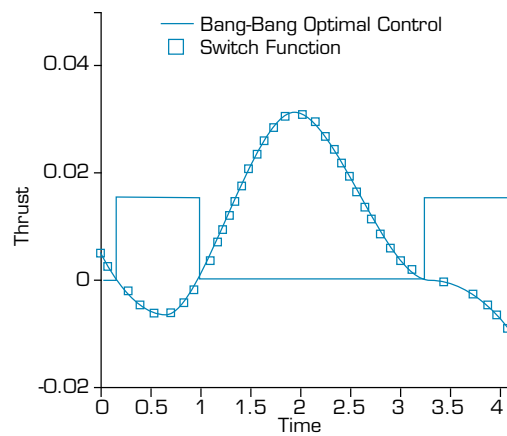
Figure 23. Non-dimensionalized tangential velocity.

In this problem, two switch points are achieved. Results of state equations are compared with results to validate the operation of the mentioned method in the Figs. 20–27. These figures show that the boundary conditions are satisfied exactly. Moreover, optimal control and switch function are demonstrated in Figs. 25–27. Results show precise results of the mentioned method.



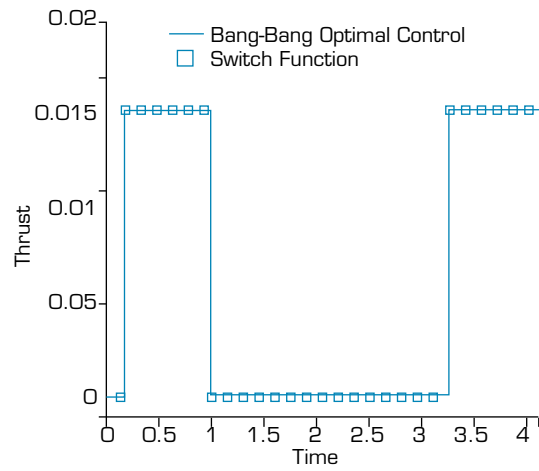
Source: Elaborated by the authors.

Figure 24. Non-dimensionalized mass reduction.



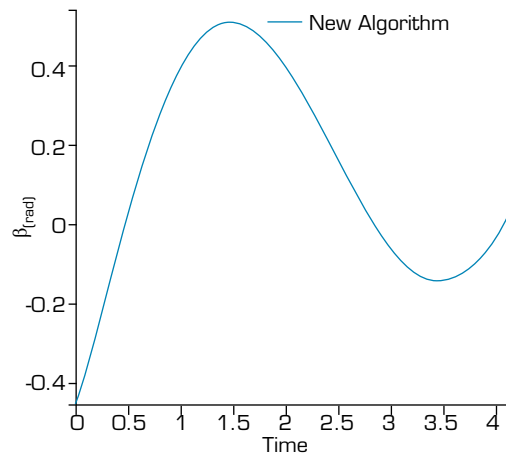
Source: Elaborated by the authors.

Figure 25. Switch function and bang-bang thrust.



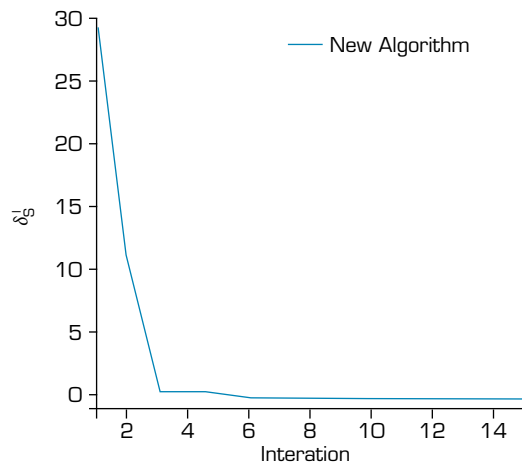
Source: Elaborated by the authors.

Figure 26. Non-dimension alized bang-bang thrust.



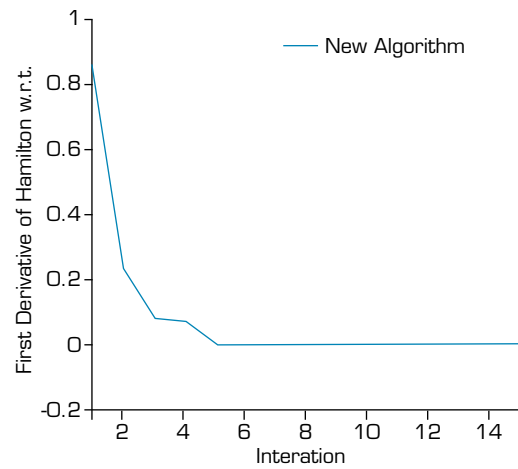
Source: Elaborated by the authors.

Figure 27. Thrust vector angle.



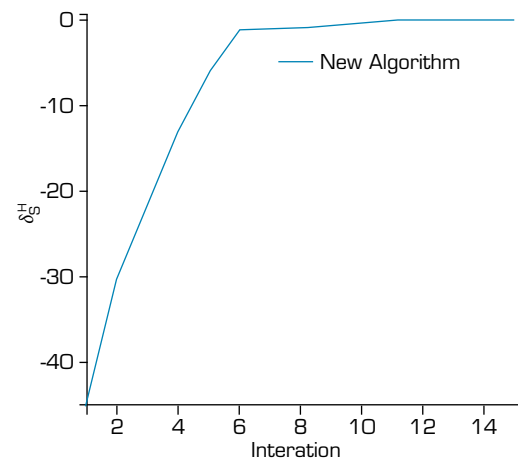
Source: Elaborated by the authors.

Figure 28. Reduction of δ_s^I .



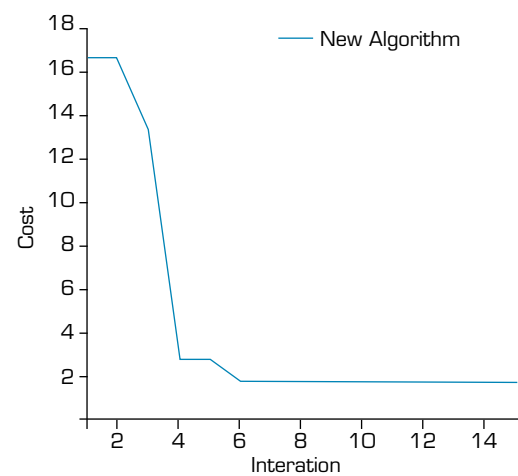
Source: Elaborated by the authors.

Figure 29. Reduction of the Hamiltonian w.r.t β, δ_u .



Source: Elaborated by the authors.

Figure 30. Reduction of δ_s^H .



Source: Elaborated by the authors.

Figure 31. Reduction of the total cost function.

All δ criteria act dynamically to enhance the robustness of the δ method and they are converging rapidly and precisely. In this problem, there are two optimal controls, $\beta(t)$ is considered as continuous control and the other as the bang-bang thruster (bang-bang optimal controller for fuel consumption) namely discontinuous optimal control. Based on the δ method, δ_u for continuous optimal controls (regarding satisfying necessary condition of optimality $\partial H(t)/(\partial u=0)$) are considered and should be minimized to zero. Figures 28–30 show the components of the criteria vector $\delta' = [\delta_s^I \delta_u \delta_s^H]$ that are converging to zero rapidly. Therefore, the novel-introduced principles in this method are satisfied precisely. Also, Fig. 31 shows the rapid converging of the total cost function in the 6th iteration and it is one of the advantages of this method. Results as the switch function (for constrained control) and thrust direction (unconstrained control) are achieved in Eqs. 40 and 41. It should be noted, the mentioned asteroid rendezvous has non-linear equations with multi-input controls.

$$f_s(t) = 2.2034 \cos(0.79949 t) - 1.3453 \sin(2.3985 t) - 1.2126 \cos(2.3985 t) - 0.84609 \cos(1.599 t) + 0.86052 \cos(3.198 t) + 3.1389 \sin(0.79949 t) - 2.9843 \sin(1.599 t) \quad (40)$$

$$\beta(t) = 0.3049 \sin(0.2695 t) + 0.63974 \sin(0.53901 t) - 0.073417 \sin(1.078 t) + 0.57016 \sin(1.3475 t) - 0.020263 \sin(0.80851 t) - 0.4608 \quad (41)$$

Low thrust Orbital Transfer

The proposed method as δ has been able to overcome the complex non-linear free and fix-final-time problems. In the following, the problem of the optimal orbital transfer, which is a completely complex problem with nonlinear equations, is considered regarding orbital parameters. The mentioned orbit transfer is considered a continuous orbital transfer from LEO to GEO. The thrust force is expressed in terms of the Eqs. 42–44 three-dimensionally based on two control angles $\psi(t)$, $\varphi(t)$ and an on-off thruster.

$$q = Th \sin \sin (\varphi(t)) \quad (42)$$

$$s = Th \cos \cos (\varphi(t)) \cos \cos (\psi(t)) \quad (43)$$

$$w = Th \cos \cos (\varphi(t)) \sin \sin (\psi(t)) \quad (44)$$

In the Eqs. 42–44, three components of the thrust vector are demonstrated as q , s and w . Also, Th is the magnitude of the thruster. The Eqs. 45–52 modified equatorial are used to solve the mentioned problem where $u(t) = [q(t) s(t) w(t)]$.

$$\frac{dP(t)}{dt} = \frac{2Th}{m(t)} \left(\sqrt{\frac{P^3(t)}{\mu_0}} \right) \frac{s(t)}{Z(t)} \quad (45)$$

$$\frac{de_x(t)}{dt} = \frac{Th}{m(t)} \sqrt{\frac{P(t)}{\mu_0}} \frac{1}{Z(t)} [Z(t) \sin \sin (L(t)) q(t) + A_1(t)s(t) - e_y(t)(h_x(t) \sin \sin (L(t)) - h_y(t) \cos \cos (L(t)))w(t)] \quad (46)$$

$$\frac{de_x(t)}{dt} = \frac{Th}{m(t)} \sqrt{\frac{P(t)}{\mu_0}} \frac{1}{Z(t)} [-Z(t) \cos \cos (L(t)) q(t) + A_2(t)s(t) + e_x(t)(h_x(t) \sin \sin (L(t)) - h_y(t) \cos \cos (L(t)))w(t)] \quad (47)$$

$$\frac{dh_x(t)}{dt} = \frac{Th}{2m(t)} \sqrt{\frac{P(t) X(t)}{\mu_0 Z(t)}} \cos \cos (L(t)) w(t) \quad (48)$$

$$\frac{dh_y(t)}{dt} = \frac{Th}{2m(t)} \sqrt{\frac{P(t) X(t)}{\mu_0 Z(t)}} \sin \sin (L(t)) w(t) \quad (49)$$

$$\frac{dL(t)}{dt} = \sqrt{\frac{\mu_0}{P^3(t)}} Z^2(t) + \frac{1}{m(t)} \sqrt{\frac{P(t)}{\mu_0}} \frac{1}{Z(t)} [(h_x(t) \sin \sin (L(t)) - h_y(t) \cos \cos (L(t))) w(t)] \quad (50)$$

$$\frac{dm(t)}{dt} = -\frac{Th}{I_{sp} g_0} \|(q(t), s(t), w(t))\| \quad (51)$$

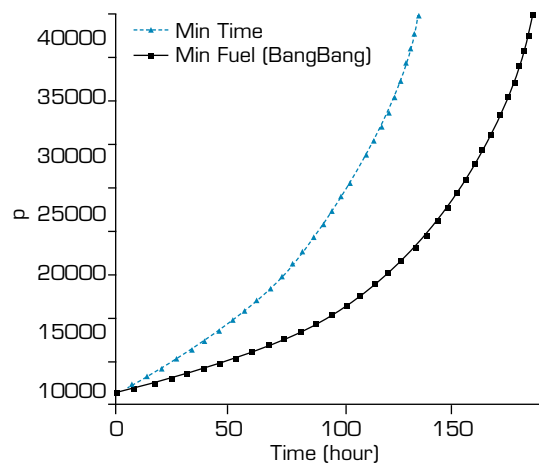
$$\begin{aligned} \{Z(t) = 1 + e_x(t) \cos \cos (L(t)) + e_y(t) \sin \sin (L(t)) \quad A_1(t) = e_x(t) + (1 + Z(t)) \\ \cos \cos (L(t)) \quad A_2(t) = e_y(t) + (1 + Z(t)) \sin \sin (L(t)) \quad X(t) = 1 + h_x^2(t) + h_y^2(t) \end{aligned} \quad (52)$$

which $P(t)$, $e_x(t)$, $e_y(t)$, $h_x(t)$, $h_y(t)$, $L(t)$, $m(t)$ are state variables in the modified equatorial coordinate. The boundary conditions of the problem are also considered as follows (Eqs. 53 and 54) regarding orbital elements as semi-major axes, eccentricity, inclination, the argument of periapsis, the longitude of the ascending node, true anomaly, and mass. It should be noted that two boundary conditions, true anomaly and mass, are considered free at the final.

$$I.C\{a = 10000km, e = 0.186, i = 25, \omega = 0, \Omega = -90, \theta = 90, m = 1000kg\} \quad (53)$$

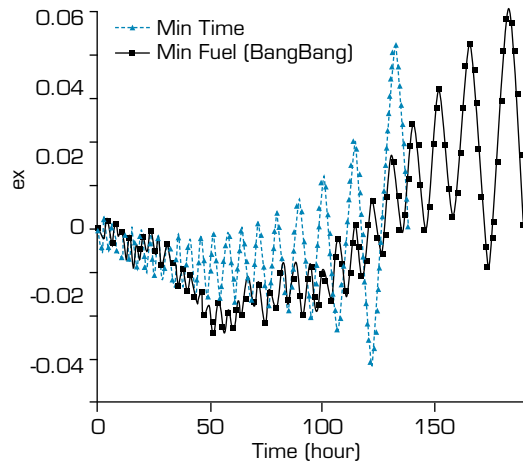
$$F.C\{a = 42000km, e = 0, i = 0, \omega = -90, \Omega = 0, \theta = free, m = free\} \quad (54)$$

Two main cost functions minimum-time and minimum-fuel are considered. Results are obtained by the optimal on-off switching thruster. This on-off thruster can operate in space by two un constrained control angles $\psi(t)$, $\varphi(t)$ and bring the space vehicle to its final destination. Therefore, the mentioned optimal control problem is considered with three controls, with respect to one on-off thruster and two un constrained controls. Figures 32–36 describe the state variables in the modified equatorial coordinate regarding the two mentioned main cost functions.



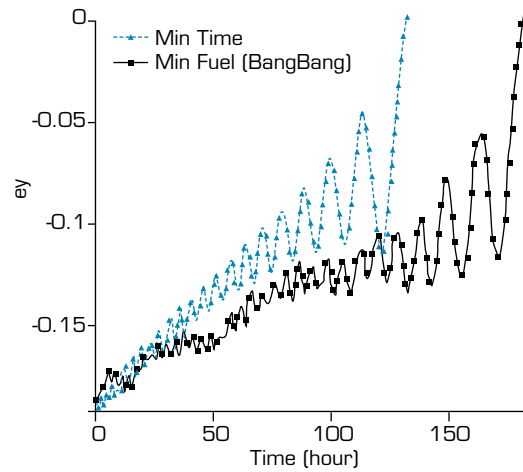
Source: Elaborated by the authors.

Figure 32. Time history of $P(t)$ minimum-time and minimum-fuel.



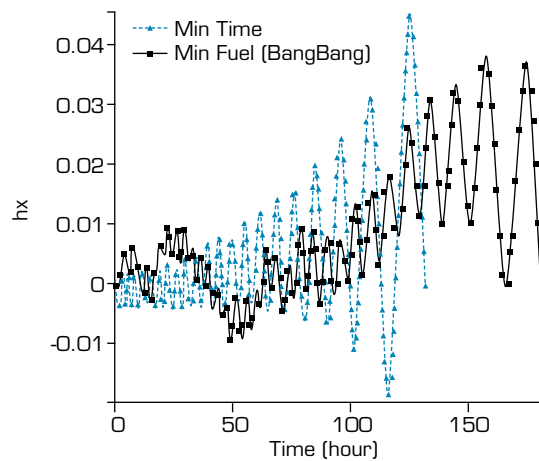
Source: Elaborated by the authors.

Figure 33. Time history of $e_x(t)$, minimum-time and minimum-fuel.



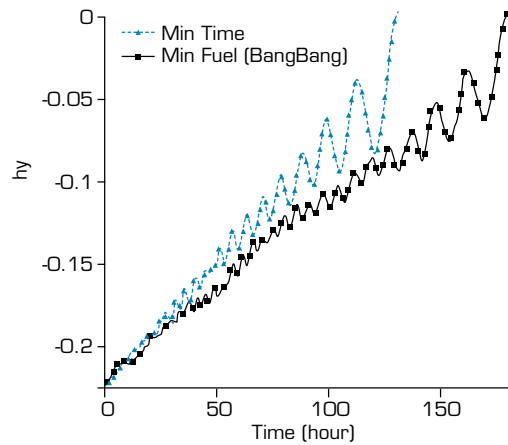
Source: Elaborated by the authors.

Figure 34. Time history of $e_y(t)$, minimum-time and minimum-fuel.



Source: Elaborated by the authors.

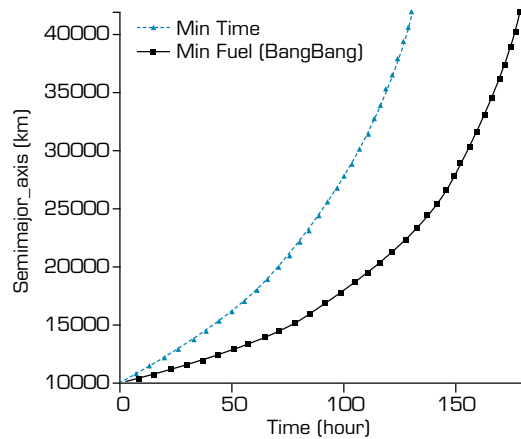
Figure 35. Time history of $h_x(t)$, minimum-time and minimum-fuel.



Source: Elaborated by the authors.

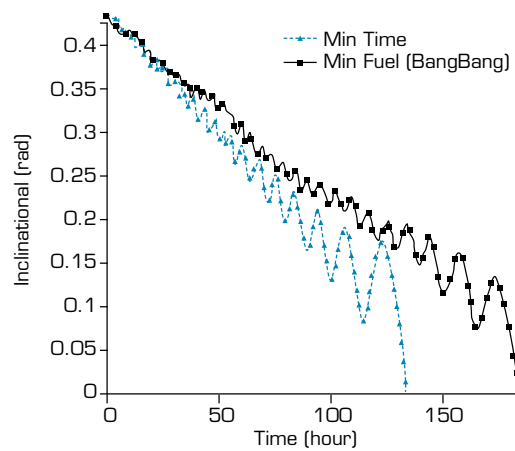
Figure 36. Time history of $h_y(t)$, minimum-time and minimum-fuel.

In order to better understand the spacecraft motion, time histories of the state variables are illustrated in the form of semi-major axes, inclination, eccentricity, longitude of ascending node, and argument of periapsis in Figs. 37–41.



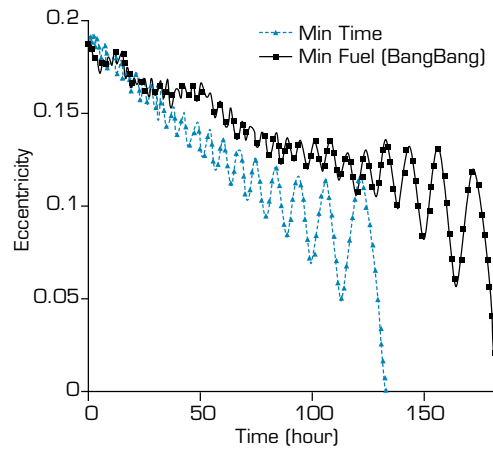
Source: Elaborated by the authors.

Figure 37. Time history of semi major, minimum-time and minimum-fuel.



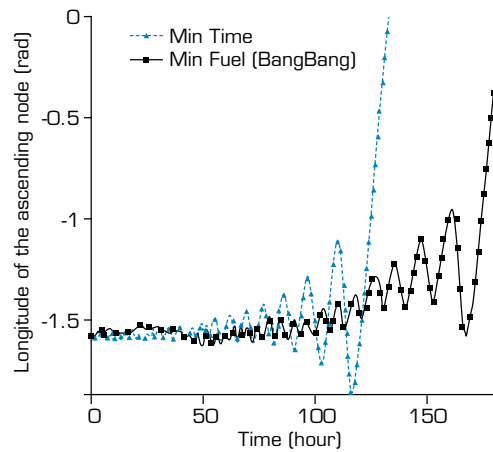
Source: Elaborated by the authors.

Figure 38. Time history of inclination, minimum-time and minimum-fuel.



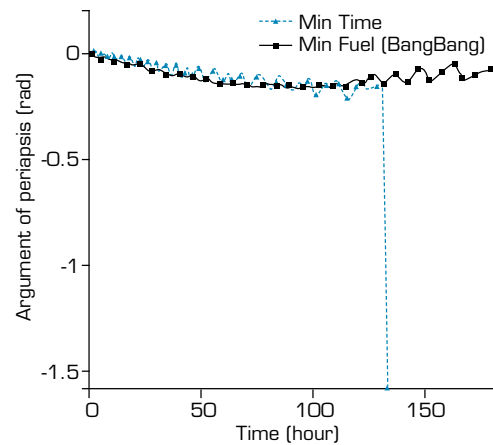
Source: Elaborated by the authors.

Figure 39. Time history of eccentricity, minimum-time and minimum-fuel.



Source: Elaborated by the authors.

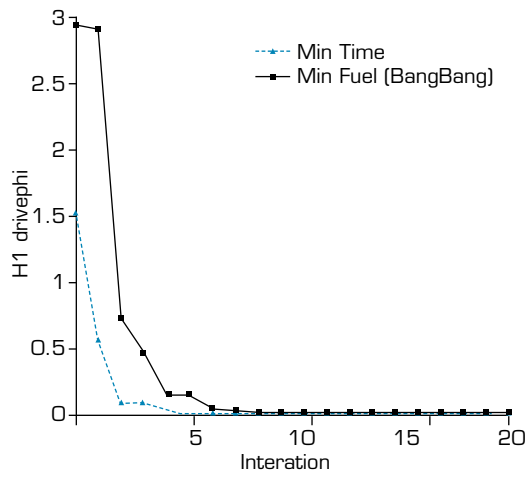
Figure 40. Time history of longitude of the ascending node, minimum-time and minimum-fuel.



Source: Elaborated by the authors.

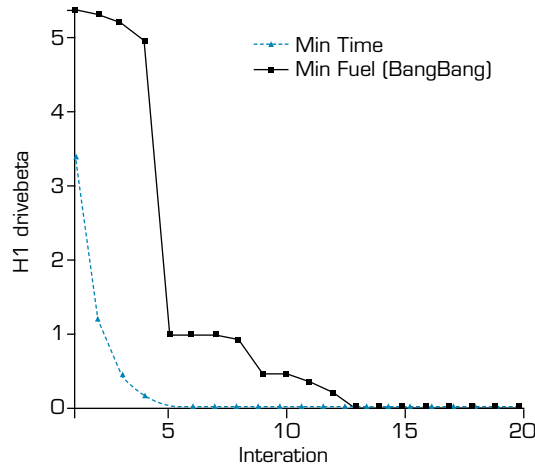
Figure 41. Time history of argument of periapsis, minimum-time and minimum-fuel.

Since two control angles $\psi(t)$, $\varphi(t)$ are unconstrained, the following optimality conditions $(\partial H(t))/(\partial \psi(t))=0$, $(\partial H(t))/(\partial \varphi(t))=0$ can be considered, and the δ parameters as δ_1 , δ_1' are minimized to zero (see Figs. 42 and 43).



Source: Elaborated by the authors.

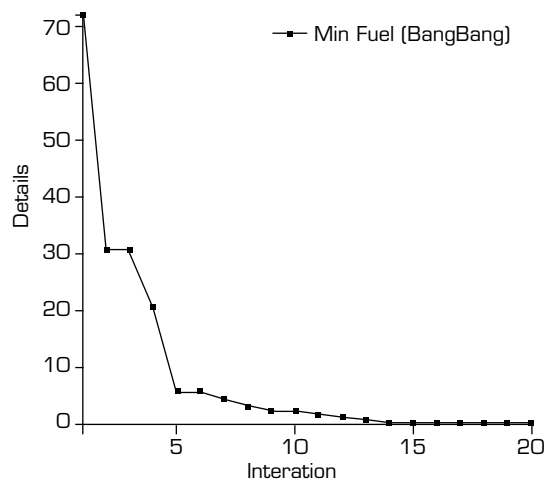
Figure 42. Reduction of $\partial H/\partial \psi$ or δ_1 to zero, minimum-time and minimum-fuel.



Source: Elaborated by the authors.

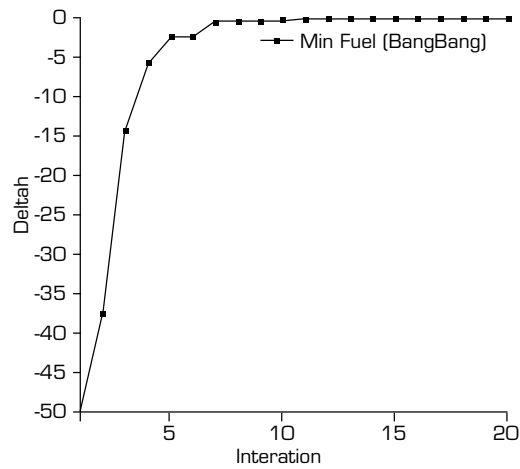
Figure 43. Reduction of $\partial H/\partial \psi$ or δ_2 to zero, minimum-time and minimum-fuel.

Furthermore, other δ parameters as δ_s^I , δ_s^H are minimized to zero and sketched in Figs. 44 and 45.



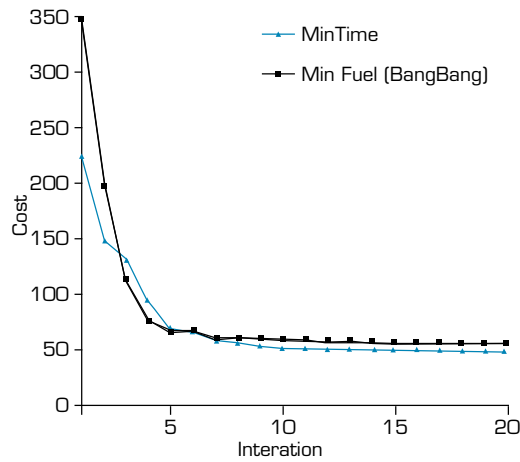
Source: Elaborated by the authors.

Figure 44. Reduction of δ_s^I to zero, minimum-fuel.



Source: Elaborated by the authors.

Figure 45. Reduction of δ_s^H to zero, minimum-fuel.

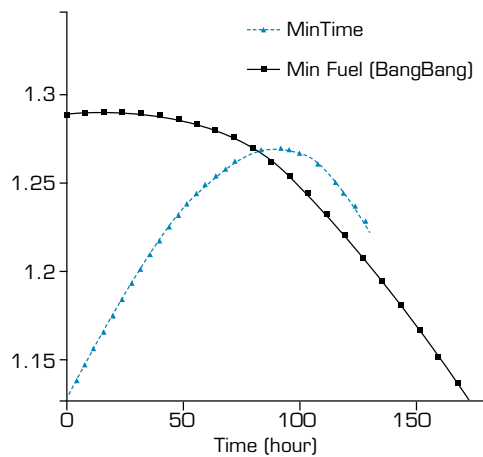


Source: Elaborated by the authors.

Figure 46. Reduction of the main criteria, minimum-time and minimum-fuel.

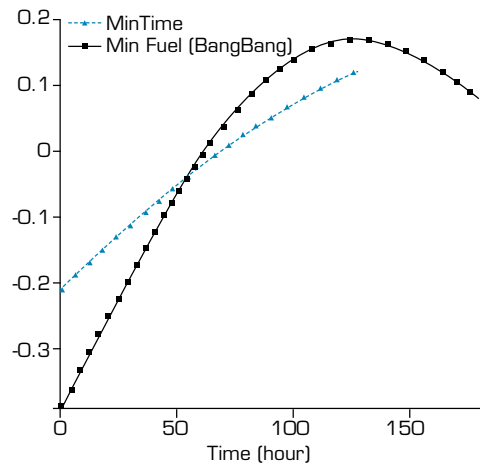
Figures 42–45 show how δ parameters are minimized to zero precisely. Also, indicate that the δ method principles are well satisfied.

Figures 47 and 48 demonstrate the time history of two unconstrained optimal control angles $\psi(t), \varphi(t)$ for minimum-time and minimum-fuel.



Source: Elaborated by the authors.

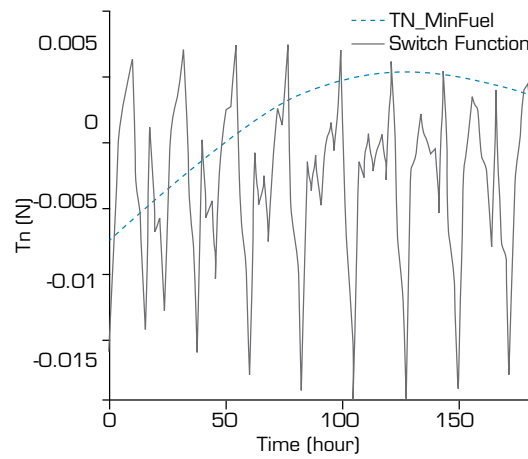
Figure 47. Time history of optimal control angle $\psi(t)$ (rad).



Source: Elaborated by the authors.

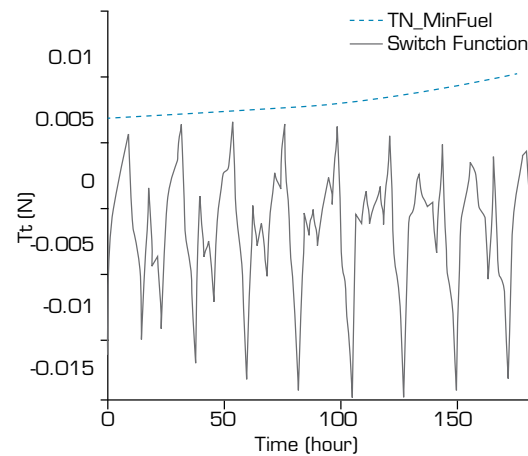
Figure 48. Time history of optimal control angle $\varphi(t)$ (rad).

Next, figures of three elements $u^\gamma(t) = [q(t) \ s(t) \ w(t)]$ as tangential thrust, radial thrust and normal thrust, and their switch functions for minimum-fuel criterion, (bang-bang control) are demonstrated in Figs. 49 and 50.



Source: Elaborated by the authors.

Figure 49. Time history of optimal bang-bang control, normal thrust.



Source: Elaborated by the authors.

Figure 50. Time history of optimal bang-bang control, tangential thrust.

Results of the switch function for constrained control and two un constrained control angles $\psi(t)$, $\varphi(t)$ for minimum-fuel criterion are illustrated in Eqs. 55–57 regarding the Fourier series and GA-PSO optimizer.

$$f_s = 12.566\sin(0.00071638t) - 1.7844\cos(0.00071638t) - 5.3316\cos(0.00023879t) \\ + 9.6418\cos(0.00047759t) - 12.517\cos(0.00095518t) - 4.2014\sin(0.00023879t) \\ - 4.8337\sin(0.00047759t) + 6.884\sin(0.00095518t) - 12.343 \quad (55)$$

$$\psi(t) = 0.52421\sin(2.0876e - 6t) + 0.87521\sin(6.9588e - 7t) - 0.60766\sin(1.3918e - 6t) \\ - 1.1421\sin(2.7835e - 6t) + 0.67323\sin(3.4794e - 6t) + 1.2892 \quad (56)$$

$$\varphi(t) = 1.5255\sin(6.9588e - 7t) - 1.2402\sin(2.0876e - 6t) + 0.79965\sin(1.3918e - 6t) \\ - 0.40637\sin(2.7835e - 6t) + 1.002\sin(3.4794e - 6t) - 0.38893 \quad (57)$$

Also, the results of two unconstrained control angles $\psi(t)$, $\varphi(t)$ for the minimum-time criterion are illustrated in Eqs. 58 and 59.

$$\psi(t) = 0.91884\sin(2.2184e - 6t) + 0.33283\sin(1.331e - 6t) - 1.1953\sin(4.4367e - 7t) \\ + 0.96718\sin(8.8735e - 7t) - 1.0808\sin(1.7747e - 6t) - 0.21112 \quad (58)$$

$$\varphi(t) = 1.5663\sin(2.2184e - 6t) - 1.2057\sin(1.331e - 6t) - 1.0502\sin(4.4367e - 7t) \\ - 0.76108\sin(8.8735e - 7t) - 0.036293\sin(1.7747e - 6t) + 1.1282 \quad (59)$$

In Table 3, the GA-PSO optimizer parameters are presented for the two mentioned problems.

Table 3. GA-PSO optimizer parameters.

GA-PSO Parameters	
Population Size	5000
Keep Percent	40/100
Cross Percent	40/100
Mutation Percent	5/100
Selection Mode	Tournament Selection

Source: Elaborated by the authors.

Table 4 summarizes the final-time of minimum-time and minimum-fuel criteria. From the results, the reduction of final-time in the problem of the min-time is clear, but the fuel consumption is higher in front of the minimum-fuel criterion. The above problem is a complex non-linear problem in space missions and trajectory design, which provides precise results based on the δ method. Regarding the solved problems, the δ method can be considered a novel and innovative solution in the field of constrained and un constrained non-linear problems. Also, optimal controls can be achieved simply in the form of time series. Therefore, the mentioned method can be presented to space mission designers as an efficient method with desirable accuracy.

Table 4. Comparing final-time and fuel consumption for min-time and min-fuel criteria.

Min Time		Min Fuel	
Final Time	5.4926 (day)	Final Time	7.5538 (day)
Fuel Consumption	0.6952 (kg)	Fuel Consumption	0.6771 (Kg)

Source: Elaborated by the authors.

CONCLUSION

In this work, a novel method named as δ method for constrained and un constrained optimal control problems is introduced. The mentioned method investigated space trajectory problems. This novel method does not need any initial guess and has high-speed convergence with the aid of heuristic optimization techniques such as GA-PSO and imperialist competition algorithm, orthogonal functions (Fourier, Chebyshev, and Legendre), and the principles of the optimal control theory. Regarding the introduced method, three case studies of soft Lunar landing, asteroid rendezvous, and low-thrust orbit transfer are considered to solve this method. Two powerful optimization techniques (GA-PSO and imperialist competition algorithm) and the three orthogonal functions (Fourier, Chebyshev, and Legendre) have precise results. However, from processing time and converging speed, the combination of the Fourier series and GA-PSO optimizer is the candidate. Regarding the approximation of the optimal control, new augmented criteria based on the optimal control theory were introduced to minimize the optimization techniques. The main criterion (such as minimum-time or minimum-fuel) was added by new criteria introduced by δ based on the necessary and sufficient conditions in the optimal control theory to improve the precision and simple achievement of the results. One of the advantages of this study belonged to the independence of the proposed δ method to the initial guesses. Emphasizing the minimum-time and minimum-fuel criteria and different space missions show the ability of this method for different types of optimal control problems. From processing time and rapidly converging, the combination of the Fourier series and the GA-PSO optimizer is a candidate. Also, the vectors of optimization variables are achieved in the defined ranges. Furthermore, the results show that the boundary conditions are satisfied exactly. All δ criteria act dynamically to enhance the robustness of the δ method and they are converging rapidly and precisely. It should be noted, the mentioned method overcomes the non-linear equations with multi-input controls. Moreover, the achieved results show the accuracy and simplicity of this new method versus common complicated methods in optimal control theory. So, it will be a novel method for space mission analyzers and designers for future studies.

CONFLICT OF INTEREST

The authors declare no conflict of interest.

DATA AVAILABILITY STATEMENT

All data sets were generated or analyzed in the current study.

FUNDING

Not applicable.

ACKNOWLEDGEMENTS

The author acknowledges with grateful appreciation the kind assistance provided by Professor A. B. Novinzadeh for his Research at the K. N. Toosi University of Technology.

REFERENCES

- Abdollahi M, Isazadeh A, Abdollahi D (2013) Imperialist competitive algorithm for solving systems of nonlinear equations. *Comput Math Appl* 65(12):1894-1908. <https://doi.org/10.1016/j.camwa.2013.04.018>
- AlandiHallaj MA, Assadian N (2019) Asteroid precision landing via Probabilistic Multiple-Horizon Multiple-Model Predictive Control. *Acta Astronaut* 161:531-541. <https://doi.org/10.1016/j.actaastro.2019.04.009>
- Ardalan Z, Karimi S, Poursabzi O, Naderi B (2015) A novel imperialist competitive algorithm for generalized traveling salesman problems. *Appl Soft Comput* 26:546-555. <https://doi.org/10.1016/j.asoc.2014.08.033>
- Bazzocchi MCF, Emami MR (2018) Stochastic optimization of asteroid three-dimensional trajectory transfer. *Acta Astronaut* 152:705-718. <https://doi.org/10.1016/j.actaastro.2018.09.009>
- Ben-Asher J-Z (2010) *Optimal Control Theory with Aerospace Applications*. Reston: AIAA. <https://doi.org/10.2514/4.867347>
- Binfeng P, Yangyang M, Yang N (2019) A new fractional homotopy method for solving nonlinear optimal control problems. *Acta Astronaut* 161:12-23. <https://doi.org/10.1016/j.actaastro.2019.05.005>
- Braun V, Klinkrad H, Stoll E (2016) Orbit Information of Predetermined Accuracy and its Sharing in the SST Context. Paper presented at AIAA/AAS Astrodynamics Specialist Conference. ARC; Long Beach, California. <https://doi.org/10.2514/6.2016-5657>
- Chai R, Liu D, Liu T, Tsourdos A, Xia Y, Chai S (2022c) Deep Learning-Based Trajectory Planning and Control for Autonomous Ground Vehicle Parking Maneuver. *IEEE Trans Autom Sci Eng* 1-15. <https://doi.org/10.1109/TASE.2022.3183610>
- Chai R, Niu H, Carrasco J, Arvin F, Yin H, Lennox B (2022) Design and Experimental Validation of Deep Reinforcement Learning-Based Fast Trajectory Planning and Control for Mobile Robot in Unknown Environment. *IEEE Trans Neural Networks Learn Syst* 1-15. <https://doi.org/10.1109/TNNLS.2022.3209154>
- Chai R, Tsourdos A, Gao H, Chai S, Xia Y (2022e) Attitude tracking control for reentry vehicles using centralised robust model predictive control. *Automatica* 145:110561. <https://doi.org/10.1016/j.automatica.2022.110561>
- Chai R, Tsourdos A, Gao H, Xia Y, Chai S (2022d) Dual-Loop Tube-Based Robust Model Predictive Attitude Tracking Control for Spacecraft with System Constraints and Additive Disturbances. *IEEE Trans Ind Electron* 69(4):4022-4033. <https://doi.org/10.1109/TIE.2021.3076729>
- Chai R, Tsourdos A, Savvaris A, Chai S, Xia Y, Chen CLP (2022b) Design and Implementation of Deep Neural Network-Based Control for Automatic Parking Maneuver Process. *IEEE Trans Neural Networks Learn Syst* 33(4):1400-1413. <https://doi.org/10.1109/TNNLS.2020.3042120>
- Chai R, Tsourdos A, Savvaris S, Chai S, Xia Y, Chen CLP (2021) Multiobjective Overtaking Maneuver Planning for Autonomous Ground Vehicles. *IEEE Trans Cybern* 51(8):4035-4049. <https://doi.org/10.1109/TCYB.2020.2973748>
- Chen N, Wang Y, Yang D-H (2018) Time-varying bang-bang property of time optimal controls for heat equation and its application. *Syst Control Lett* 112:18-23. <https://doi.org/10.1016/j.sysconle.2017.12.008>

- Chen Z, Tang S (2018) Neighboring optimal control for open-time multiburn orbital transfers. *Aerosp Sci Technol* 74:37-45. <https://doi.org/10.1016/j.ast.2018.01.003>
- Fuica F, Otárola E, Salgado AJ (2019) An a posteriori error analysis of an elliptic optimal control problem in measure space. *Comput Math Appl* 77(10):2659-2675. <https://doi.org/10.1016/j.camwa.2018.12.043>
- Gao Y, Lu X, Peng Y, Xu B, Zhao T (2019) Trajectory optimization of multiple asteroids exploration with asteroid 2010TK₇ as main target. *Adv Space Res* 63(1):432-442. <https://doi.org/10.1016/j.asr.2018.08.047>
- Han H, Qiao D, Chen H, Li X (2019) Rapid planning for aerocapture trajectory via convex optimization. *Aerosp Sci Technol* 84:763-775. <https://doi.org/10.1016/j.ast.2018.11.009>
- Henrion D, Kružík M, Weisser T (2019) Optimal control problems with oscillations, concentrations and discontinuities. *Automatica* 103:159-165. <https://doi.org/10.1016/j.automatica.2019.01.030>
- Henriques JCC, Lemos JL, Eça L, Gato LMC, Falcão AFO (2017) A high-order Discontinuous Galerkin Method with mesh refinement for optimal control. *Automatica* 85:70-82. <https://doi.org/10.1016/j.automatica.2017.07.029>
- Henriques JCC, Lemos JL, Eça L, Valério JNH, Gato LMC, Falcão AFO (2017) A Discontinuous Galerkin Method for optimal and sub-optimal control applied to an oscillating water column wave energy converter. *IFAC-PapersOnLine* 50(1):15670-15677. <https://doi.org/10.1016/j.ifacol.2017.08.2400>
- Kirk DE, Demetry JS (1971) *Optimal Control Theory: An Introduction. Solutions to selected problems.* Hoboken: Prentice-Hall.
- Kumar G, Kumar A, Jakka RS (2018) The particle swarm modified quasi bang-bang controller for seismic vibration control. *Ocean Eng* 166:105-116. <https://doi.org/10.1016/j.oceaneng.2018.08.002>
- Li S, Zhou Z (2019) Fractional spectral collocation method for optimal control problem governed by space fractional diffusion equation. *Appl Math Comput* 350:331-347. <https://doi.org/10.1016/j.amc.2019.01.018>
- Lunghi P (2017) *Hazard Detection and Avoidance Systems for Autonomous Planetary Landing (doctoral dissertation).* Milan: Polytechnic University of Milan. In English.
- Lykina V, Pickenhain S (2017) Weighted functional spaces approach in infinite horizon optimal control problems: A systematic analysis of hidden opportunities and advantages. *J Math Anal Appl* 454(1):195-218. <https://doi.org/10.1016/j.jmaa.2017.04.069>
- Maheri MR, Talezadeh M (2018) An Enhanced Imperialist Competitive Algorithm for optimum design of skeletal structures. *Swarm Evol Comput* 40:24-36. <https://doi.org/10.1016/j.swevo.2017.12.001>
- Mohammadi MS, Naghash A (2019) Robust optimization of impulsive orbit transfers under actuation uncertainties. *Aerosp Sci Technol* 85:246-258. <https://doi.org/10.1016/j.ast.2018.11.026>
- Naidu DS (2003) *Optimal control systems.* Boca Raton: CRC Press.
- Pontani M, Cecchetti G, Teofilatto P (2015) Variable-time-domain neighboring optimal guidance applied to space trajectories. *Acta Astronaut* 115:102-120. <https://doi.org/10.1016/j.actaastro.2015.05.020>
- Quarta AA, Mengali G (2019) Simple solution to optimal cotangential transfer between coplanar elliptic orbits. *Acta Astronaut* 155:247-254. <https://doi.org/10.1016/j.actaastro.2018.12.007>
- Rabiee A, Sadeghi M, Aghaei J (2018) Modified imperialist competitive algorithm for environmental constrained energy management of microgrids. *J Clean Prod* 202:273-292. <https://doi.org/10.1016/j.jclepro.2018.08.129>

Ross IM (2015) A Primer on Pontryagin's Principle in Optimal Control. San Francisco: Collegiate Publishers.

Ross IM (2019). An optimal control theory for accelerated optimization. ArXiv preprint arXiv:1902.09004. [accessed 2019 Feb. 24]. <https://arxiv.org/abs/1902.09004>

Shafieenejad I, Novinzadeh AB (2010) Closed form optimal continuous guidance scheme for new dynamic of electrical propulsion plane change transfers. Proc Inst Mech Eng Part K J Multi-body Dyn 224(2):233-241. <https://doi.org/10.1243/14644193JMBD235>

Shafieenejad I, Novinzadeh AB, Molazadeh VR (2014) Comparing and analyzing min-time and min-effort criteria for free true anomaly of low-thrust orbital maneuvers with new optimal control algorithm. Aerosp Sci Technol 35:116-134. <https://doi.org/10.1016/j.ast.2014.03.009>

Shafieenejad I, Novinzadeh AB, Molazadeh VR (2015) Introducing a novel algorithm for minimum-time low-thrust orbital transfers with free initial condition. Proc Inst Mech Eng Part G J Aerosp Eng 229(2):333-351. <https://doi.org/10.1177/0954410014533311>

Shirazi A, Ceberio J, Lozano JA (2018) Spacecraft trajectory optimization: A review of models, objectives, approaches and solutions. Progress in Aerospace Sciences 102:76-98. <https://doi.org/10.1016/j.paerosci.2018.07.007>

Udupa G, Sundaram G, Poduval P, Aditya AP, Pillai K, Kumar N, Shaji N, Nikhil PC, Ramacharan P, Rajan SS (2018) Certain Investigations on Soft Lander for Lunar Exploration. Procedia Comput Sci 133:393-400. <https://doi.org/10.1016/j.procs.2018.07.048>

Yan H, Zhu Y (2015) Bang-bang control model for uncertain switched systems. Appl Math Model 39(10-11):2994-3002. <https://doi.org/10.1016/j.apm.2014.10.042>

Zhu Z, Gan Q, Yang X, Gao Y (2017) Solving fuel-optimal low-thrust orbital transfers with bang-bang control using a novel continuation technique. Acta Astronaut 137:98-113. <https://doi.org/10.1016/j.actaastro.2017.03.032>